Near-Ultraviolet Evanescent-Wave Absorption Sensor Based on a Multimode Optical Fiber

ARTICLE *in* ANALYTICAL CHEMISTRY · MAY 1998

Impact Factor: 5.64 · DOI: 10.1021/ac970942v · Source: PubMed

3 AUTHORS, INCLUDING:

Radislav A. Potyrailo
General Electric
158 PUBLICATIONS **2,844** CITATIONS
SEE PROFILE

Gary M. Hieftje
Indiana University Bloomington
612 PUBLICATIONS **10,686** CITATIONS
SEE PROFILE

Anal. Chem. **1998,** *70,* 1639−1645

Technical Notes

Near-Ultraviolet Evanescent-Wave Absorption Sensor Based on a Multimode Optical Fiber

Radislav A. Potyrailo,[†] Steven E. Hobbs,[‡] and Gary M. Hieftje*

Department of Chemistry, Indiana University, Bloomington, Indiana 47405

Fiber-optic near-ultraviolet evanescent-wave sensors have been constructed, and their feasibility for practical applications has been demonstrated. The sensors, used for the detection of ozone near the 254-nm peak of the Hartley absorption band, were fabricated from coiled segments of low-cost multimode plastic-clad silica optical fibers. The sensing sections were produced alternatively by stripping only the protective jacket from the fiber to expose the gas-permeable silicone cladding or by stripping the jacket and the cladding to expose the bare-silica fiber core. Response characteristics are given, including sensitivity to ozone, reversibility, and aging effects. The useful lifetime was unacceptably short for the sensor that employed the bare-silica core, whereas the exposed-cladding sensor demonstrated good stability over the entire two-month period of investigation. The latter, more useful sensor demonstrated a linear response to ozone over the range 0.02−0.35 vol % and a reversible response with a time constant on the order of 1 min. Differences in ozone absorption spectra obtained in the transmission and evanescent-wave modes are discussed. Projected applications of the new exposed-cladding sensor include ozone determination in water-treatment processes and ozone production plants.

Attenuated total reflection (ATR) spectroscopy is a well-established technique for chemical analysis.[1] The technique is based on the penetration of an evanescent wave into an absorbing sample. The amount of evanescent wave absorption is directly proportional to both the number of reflections within the ATR waveguide and the penetration depth of the evanescent field in the sample medium. The latter, in turn, is directly proportional to the wavelength of the probing radiation.[1] Thus, when it is possible, a long wavelength of probing radiation should be used to compensate for the small number of reflections in a conventional ATR element. The use of multiple-reflection ATR elements in the near-ultraviolet (UV)[2] and visible[3,4] spectral ranges is ordinarily limited to the determination of species with molar absorptivities of at least 10^4 M^{-1} cm^{-1}.

A multimode optical fiber is a particularly useful ATR element because its relatively narrow core diameter provides a large number of internal reflections per unit length.[5] In addition, a sensing optical fiber can be several orders of magnitude longer than a conventional bulk multiple-reflection ATR element.[6] These attractive advantages have motivated investigations of evanescent-wave fiber-optic chemical sensors which operate in the middle infrared (IR),[7,8] near-IR,[9−11] and visible[12−14] spectral regions.

Many species of analytical interest can be detected by evanescent-wave absorption with a sensor based on a plastic-clad silica (PCS) optical fiber with an exposed (but not removed) cladding. The silicone cladding of a conventional PCS fiber provides a protective layer over the optical interface and is selectively permeable to neutral species. Spectroscopic sensors based on optical fibers with an exposed silicone cladding have been used for the near-IR detection of organic solvents[9−11] and for visible-wavelength measurement of organic dyes dissolved in nonpolar solvents.[12,13] To date, there are no published reports on fiber-optic sensors for evanescent-wave sensing in the near-UV region.[15]

[†] Present address: Characterization and Environmental Technology Laboratory, Corporate Research and Development, General Electric Co., Building K-1, P.O. Box 8, Schenectady, NY, 12301.

[‡] Present address: Nellcor Puritan Bennett, 4280 Hacienda Drive, Pleasanton, CA 94588.

(1) Mirabella, F. M., Jr., Ed. *Internal reflection spectroscopy: Theory and applications*; Practical Spectroscopy 15; Marcel Dekker: New York, 1993.
(2) Danielsson, L.-G.; Sheng, C. X. *Process Control Qual.* **1994**, *6*, 149−157.
(3) Hansen, W. N. *Anal. Chem.* **1963**, *35*, 765−766.
(4) Hansen, W. N.; Horton, J. A. *Anal. Chem.* **1964**, *36*, 783−787.
(5) Ruddy, V.; MacCraith, B. D.; Murphy, J. A. *J. Appl. Phys.* **1990**, *67*, 6070−6074.
(6) Blyler, L. L., Jr.; Lieberman, R. A.; Cohen, L. G.; Ferrara, J. A.; MacChesney, J. B. *Polym. Eng. Sci.* **1989**, *29*, 1215−1218.
(7) Jakusch, M.; Mizaikoff, B.; Kellner, R.; Katzir, A. *Sens. Actuators B* **1997**, *38−39*, 83−87.
(8) Regan, F.; MacCraith, B. D.; Walsh, J. E.; Odwyer, K.; Vos, J. G.; Meaney, M. *Vib. Spectrosc.* **1997**, *14*, 239−246.
(9) DeGrandpre, M. D.; Burgess, L. W. *Appl. Spectrosc.* **1990**, *44*, 273−279.
(10) Bürck, J.; Conzen, J. P.; Ache, H. J. *Fresenius' J. Anal. Chem.* **1992**, *342*, 394−400.
(11) Blair, D. S.; Burgess, L. W.; Brodsky, A. M. *Appl. Spectrosc.* **1995**, *49*, 1636−1645.
(12) DeGrandpre, M. D.; Burgess, L. W. *Proc. SPIE-Int. Soc. Opt. Eng.* **1988**, *990*, 170−174.
(13) DeGrandpre, M. D.; Burgess, L. W. *Anal. Chem.* **1988**, *60*, 2582−2586.
(14) Deboux, B. J. C.; Lewis, E.; Scully, P. J.; Edwards, R. *J. Lightwave Technol.* **1995**, *13*, 1407−1414.
(15) Potyrailo, R. A.; Hobbs, S. E.; Hieftje, G. M. FACSS XXI Annual Meeting, 1994; Paper 857.

S0003-2700(97)00942-6 CCC: $15.00
Published on Web 03/18/1998

Yet, there are many species of analytical interest that absorb in the near-UV (180−350 nm).[16,17] Accordingly, this paper demonstrates the feasibility of near-UV evanescent-wave fiber-optic monitoring, with ozone serving as an example analyte. Ozone, which absorbs at the peak of the Hartley band at 254 nm, is considered to be one of the seven most important harmful gaseous pollutants.[18] Ozone is a toxic gas and one of the most powerful oxidants. It lowers plant productivity[19] and is recognized as a strong lung irritant.[20]

However, ozone has many practical applications. Its most widespread uses are for the treatment of drinking water and elimination of odors from industrial processes and municipal wastewater treatment plants. In addition, the manufacture of specific chemical products and pharmaceutical intermediates involves the use of ozone for carbon double-bond oxidation. Also, ozone is used for the production of camphor, sterilization of surgical equipment, purification of mineral oils and their derivatives, and bleaching clays, textile fibers, paper pulp, and sugar.[21,22]

The range of ozone concentrations to be measured in the gas phase is quite broad, varying from less than 0.01 ppm in the ambient atmosphere to 0.5 vol % in ozone contactor gases in water treatment processes, and up to 13 vol % in the gases exiting industrial ozone generators.[23] Methods of determining ozone concentrations in the gas phase include iodometric,[24] amperometric,[25] calorimetric,[26] thermal decomposition,[27] chemiluminescent,[28] fluorescent,[29] visible absorption,[30] and near-UV absorption.[31] Due to its reliability, the last method has been adopted as the reference technique to be used for calibrating other ozone measurement instruments.[32]

In this study, we combine the near-UV absorption method of ozone determination with the flexibility and convenience of the fiber-optic approach.[15] The near-UV evanescent-wave sensors were fabricated from low-cost multimode PCS optical fibers. The sensing regions were produced alternatively by stripping the cladding to expose the bare-fiber core or by stripping only a protective nylon jacket from the fiber to expose the gas-permeable silicone cladding. Both these arrangements permit evanescent-field interaction of near-UV radiation with ozone. The usefulness of the developed sensors is demonstrated in ozone determinations down to 0.02 vol % (200 ppm) required in water treatment processes and ozone production plants.

EXPERIMENTAL SECTION

Materials. A multimode PCS optical fiber was obtained from Fiberguide Industries (Superguide SPC100/200N, Stirling, NJ). The fiber consisted of a 100-μm o.d. fused-silica core, a 200-μm-o.d. cladding, and a 270-μm-o.d. nylon jacket. The cladding material is known to be an unconjugated dimethylsiloxane.[11] Propylene glycol, ethanol, and sulfuric acid used in the studies were of reagent grade.

Fiber-Optic Sensors. For these experiments, two fiber-optic sensors were constructed, one with an exposed silicone cladding and one with a bare-fiber core. The exposed-cladding sensor was prepared by removing the nylon jacket from a 180-cm-long central section of a 3-m-long fiber. The nylon jacket was removed from the cladding by immersing the fiber in boiling propylene glycol for 5 min.[13] The exposed-cladding section of the fiber was washed with ethanol, dried, coiled onto a 16-mm-diameter rod, and placed in a 0.3-L glass sample chamber. A bare-silica core sensor was prepared by removing the nylon jacket and silicone cladding from a 75-cm-long central section of a 3-m-long fiber. The nylon jacket was removed by means of the procedure described above. The silicone cladding was removed by immersing the fiber in concentrated sulfuric acid for 50 min at room temperature.[13] The unclad fiber section was washed with water and ethanol, dried, coiled onto a 50-mm-diameter rod, and placed in a 0.5-L glass sample chamber.

Instrumentation. Ozone was generated with a commercial generator (model UPS 500, Water Quality Management, Burlington, ON, Canada). The original generator design was modified to remove small air leaks by placing its UV lamp in a 3.8-cm-diameter, 30-cm-long steel tube. Brass fittings at opposite ends of the tube were used for input and output ports. Oxygen was introduced into the generator at flow rates controlled and measured by a needle valve and a rotameter, respectively. The ozone concentration from the generator was calibrated as a function of oxygen flow rate by means of a custom-made optical absorption cuvette with a 1.4-cm path length. Ozone concentrations were adjustable over the range from 0.06 to 0.35 vol % by changing the oxygen flow rate from 0.9 to 0.1 L/min.

Cuvette and evanescent-wave measurements were accomplished with the single-beam arrangement shown in Figure 1. Light from a 300-W Xe arc lamp (LS) was chopped, directed through a diaphragm (D), a set of water and neutral density filters (F), and an absorption cuvette (A) and was focused onto the entrance slit of a 0.35-m monochromator (Mono, model EU-700, GCA-McPherson, Acton, MA). The dispersed light was detected by a Hamamatsu R928 photomultiplier tube (PMT). Monochromator control and data acquisition were performed with a Macintosh computer.

After the ozone generator was calibrated by absorption in a conventional absorption cuvette (A), an optical-fiber sensor (S) was placed in the optical path between the absorption cuvette (A) and the monochromator (Mono). The light passing through the absorption cuvette was focused into the fiber input with a UV objective (O, ×15/0.28, reflecting type, Beck, England). Because

(16) Okabe, H. *Photochemistry of Small Molecules*; Wiley: New York, 1978.
(17) Hargis, L. G.; Howell, J. A.; Sutton, R. E. *Anal. Chem.* **1996**, *68*, 169R−183R.
(18) Bogue, R. W. *Environmental Sensors*; IOP Publishing Ltd., Bristol, U.K., 1993; pp 5−8.
(19) Hewitt, N.; Terry, G. *Environ. Sci. Technol.* **1992**, *26*, 1890−1891.
(20) Lippmann, M. *Environ. Sci. Technol.* **1991**, *25*, 1954−1961.
(21) *Encyclopedia of Chemical Technology*; Wiley: New York, 1981.
(22) *Gas Encyclopaedia*; Elsevier Scientific: Amsterdam, The Netherlands, 1976.
(23) Langlais, B.; Reckhow, D. A.; Brink, D. R. *Ozone in Water Treatment, Application and Engineering*; Lewis Publishers: Chelsea, MI, 1991.
(24) Saltzman, B. E.; Gilbert, N. *Anal. Chem.* **1959**, *31*, 1914−1920.
(25) Schiavon, G.; Zotti, G.; Bontempelli, G.; Farnia, G.; G., S. *Anal. Chem.* **1990**, *62*, 293−298.
(26) Maier, D. In *Ozonization Manual for Water and Wastewater Treatment*; Masschelein, W. J., Ed.; Wiley: New York, 1982.
(27) Caprio, V.; Lignola, P. G. *Anal. Chem.* **1980**, *52*, 1123−1125.
(28) Hodgeson, J. A.; Krost, K. J.; O'Keeffe, A. E.; Stevens, R. K. *Anal. Chem.* **1970**, *42*, 1795−1802.
(29) Watanabe, H.; Nakodoi, T. *J. Air Pollut. Control Assoc.* **1966**, *16*, 614−617.
(30) Fowles, M.; Wayne, R. P. *J. Phys. E: Sci. Instrum.* **1981**, *14*, 1143−1145.
(31) Bognar, J. A.; Birks, J. W. *Anal. Chem.* **1996**, *68*, 3059−3062.
(32) *1990 Annual Book of ASTM Standards*; ASTM: Philadelphia, PA, 1990; Vol. 9, Sect. 1, 731−739.

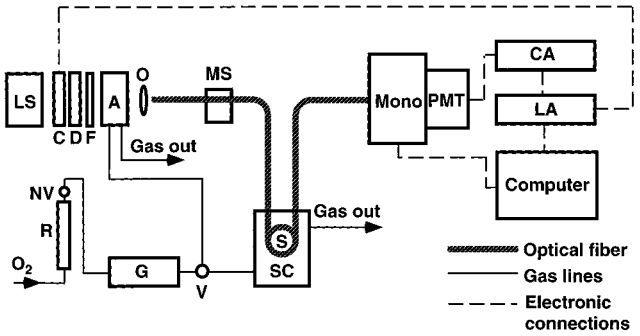

Figure 1. Experimental setup for near-UV evanescent-wave ozone detection with a multimode optical fiber: LS, light source; C, chopper; D, diaphragm; F, set of optical filters; A, absorption cuvette; O, objective; MS, mode scrambler; SC, sample chamber; S, sensor; Mono, monochromator; PMT, photomultiplier tube; CA, current amplifier; LA, lock-in amplifier; R, rotameter; NV, needle valve; V, valve; G, ozone generator.

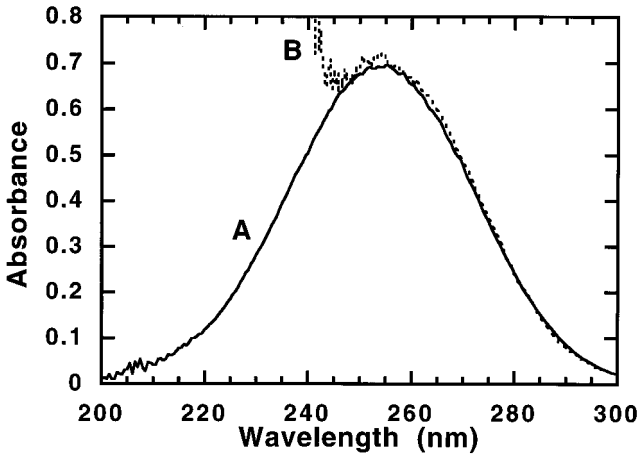

Figure 2. Absorption spectra of 0.35 vol % ozone contained within the 1.4-cm-path length absorption cuvette: (A) without and (B) with optical-fiber link (3 m long).

of the relatively short length and coiled geometry of the sensing fiber, the mode distribution was expected to be far from equilibrium.[13,33,34] To enhance the high-order mode content, thus completely filling the mode volume of the fiber, the input end of the fiber was placed in a mode scrambler (MS, model FM-1, Newport, Irvine, CA). The light transmitted through the fiber was directed into the entrance slit of the monochromator. Spectra were recorded by taking readings at 0.5-nm increments with a 1-s time constant. Scanning was initiated only after the sensor attained full response. Fixed-wavelength measurements of the steady-state and dynamic response of the sensor were performed with a 3-s time constant. During all experiments a signal drift was observed of approximately 3%/h. This drift was due to a combination of source, electronic, and temperature instability; the baseline tilt was corrected accordingly. All the measurements were performed at ambient temperature.

RESULTS AND DISCUSSION

Optical-Fiber Attenuation. The strongly wavelength-dependent light loss of the optical fiber in the near-UV required careful selection of the probe wavelength for ozone determination. Figure 2 compares the absorption spectra of 0.35 vol % ozone contained in the absorption cuvette with and without the exposed-cladding fiber used as a light guide. From Figure 2, the peak of the Hartley absorption band at 254 nm is barely visible when the optical fiber is in place. The signal-to-noise ratio (S/N) would be expected to be even worse in evanescent-wave absorption measurements because of the low evanescent-wave absorbance levels. As a result, the evanescent-wave sensors were evaluated at 265 nm, where *S/N* is considerably higher. Also, because of low *S/N*, spectra were not collected below 240 nm with the optical fibers.

Ozone Adsorption Onto Optical-Fiber Silica Core. Upon initial exposure of each sensor to a fixed ozone concentration, the output signal (transmission) rose from a low initial value to a plateau. The exposed-cladding sensor required about 15 min to stabilize, as shown in Figure 3A. Surprisingly, a much longer stabilization time was required for the sensor with the bare-silica

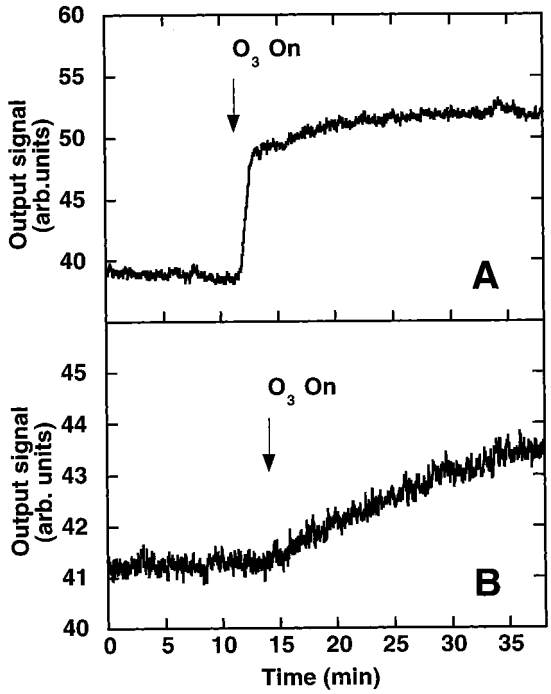

Figure 3. Temporal response of sensor at 265 nm to abrupt exposure to 0.35 vol % of ozone: (A) exposed-cladding sensor and (B) bare silica core sensor.

fiber core (Figure 3B). The upward drift of fiber transmission in Figure 3 was completely reproducible and reversible and with a recovery time of several hours (when the sensors were left overnight in air). The stabilization time became shorter at higher ozone concentrations.

The dependence of this stabilization time on ozone concentration and the long recovery time of the sensor suggest that its origin involves adsorption of ozone onto the silica core of the fiber[35] or, possibly, the oxidation of organic molecules adsorbed onto the silica surface. Similar behavior and a comparable recovery time were observed in chemiluminescent measurements of atmospheric ozone with silica gel.[28] The slow recovery time

(33) Marcuse, D. *Bell Syst. Technol. J.* **1973**, *52*, 817−842.
(34) Ruddy, V.; Shaw, G. *Appl. Opt.* **1995**, *34*, 1003−1006.
(35) Iler, R. K. *The Chemistry of Silica. Solubility, Polymerization, Colloid and Surface Properties, and Biochemistry*; Wiley-Interscience: New York, 1979.

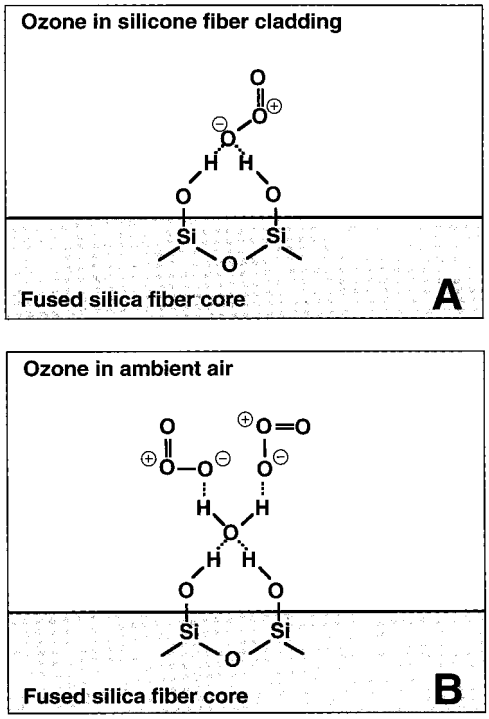

Figure 4. Illustration of ozone adsorption on silica-fiber core: (A) core protected with silicone cladding and (B) bare core in ambient (water-containing) atmosphere.

can be attributed to the slow desorption of the ozone from the silica, while the difference in stabilization time between the clad and bare-fiber sensors can be traced to the involvement of water in the adsorption process.[36]

Ozone that diffuses through the hydrophobic silicone-fiber cladding is presumably adsorbed onto a dry silica-fiber core. The resulting ozone adsorption onto the silica-fiber core is represented in Figure 4A. Previous studies indicate that two surface silanol groups can be involved in the adsorption of a single ozone molecule.[36] In contrast, adsorption of ozone onto the bare-silica fiber core can involve water vapor present in the atmosphere (see Figure 4B). In the presence of a few monolayers of water molecules present on the silica surface, each molecule of ozone is associated, on average, with about one surface silanol group.[36] The resulting adsorption and desorption are slower than in the absence of water.

Because ozone absorbs radiation at the wavelength used in this study, it might be initially seem surprising that it causes a rise rather than a drop in transmission (see Figure 3) during this stabilization period. An explanation can be found in the law that governs absorption of an evanescent wave in a multimode step-index optical fiber. When the mode volume of the fiber is filled, the absorbance A is given by[37]

$$A \approx n_2 \alpha L/(n_1 V) \qquad (1)$$

where n_1 and n_2 are the refractive indices of the fiber core and cladding, respectively, α is the absorption coefficient of the

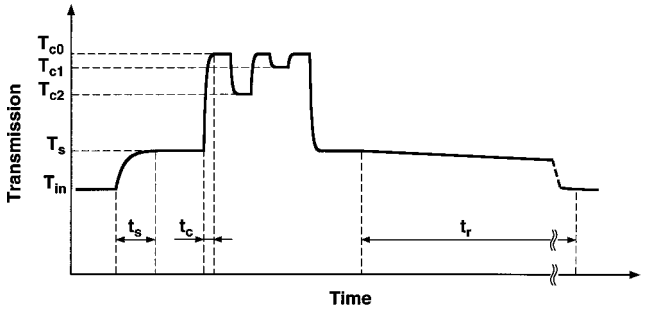

Figure 5. Conceptual representation of the variation in transmission of the fiber-optic ozone sensor during a stabilization period, sensor application, and ozone-desorption period. t_s, t_c, and t_r are the stabilization (ozone adsorption), ozone diffusion, and recovery (ozone desorption) times, respectively; T_{in} and T_s are transmission values of the sensor initially and after signal stabilization, respectively; T_{c0}, T_{c1}, and T_{c2} are the transmission values of the sensor in absence of ozone and increasing concentrations of ozone, c0 < c1 < c2. See text for details.

cladding, L is the fiber length, and V is the normalized frequency

$$V = (2\pi\rho/\lambda)(n_1^2 - n_2^2)^{1/2} \qquad (2)$$

where ρ is the radius of the fiber core and λ is the operating wavelength.

Adsorption of ozone onto the silica-fiber core clearly affects the core/cladding interface and results in both an absorption process (rise in α) and a change in refractive index (drop in n_2). In the present case, the more important effect is obviously the change in refractive index of the interface. Specifically, ozone adsorption causes n_2 to decrease at the interface and fiber transmittance, T, ($T = 10^{-A}$) to rise accordingly.

As illustrated conceptually in Figure 5, the slow kinetics of ozone desorption from the silica-fiber surface (i.e., long recovery time t_r) makes possible near-UV evanescent-wave ozone determinations after the sensor is conditioned in ozone and its signal has reached a plateau after the stabilization time t_s. During sensor stabilization, the fiber transmission rises from its initial level T_{in} to a plateau level T_s. Afterward, the presence of different concentrations of ozone causes the evanescent-wave absorption to vary. Because the latter change involves ozone diffusion and light absorption rather than chemisorption, it is faster. Also, because these small changes in ozone concentration do not cause changes at the fiber interface, the absorption factor dominates over refractive index changes, causing a loss in transmission at higher ozone concentrations. Since the recovery time t_r is much longer than the diffusion time t_c of ozone into the silicone fiber cladding, the fiber transmission T_c will depend on ozone concentration [c] as $T_c = 10^{-A_c}$, i.e., the evanescent-wave absorbance A_c will follow eq 1.

Fiber-Optic Exposed-Cladding Sensor. A calibration curve for this sensor was constructed by plotting evanescent-wave absorbance at 265 nm against ozone concentration. The evanescent-wave absorbance A was calculated as $A = \log(P_0/P)$, where P_0 is the transmitted optical power in oxygen measured immediately before or after the sensor was exposed to a particular ozone concentration and P is the transmitted optical power when the sensor attained full response in ozone. Over the tested concentra-

(36) Reimschuessel, H. K.; Mountford, G. A. *J. Colloid Interface Sci.* **1967**, *25*, 558−563.
(37) Ruddy, V. *Opt. Eng.* **1994**, *33*, 3891−3894.

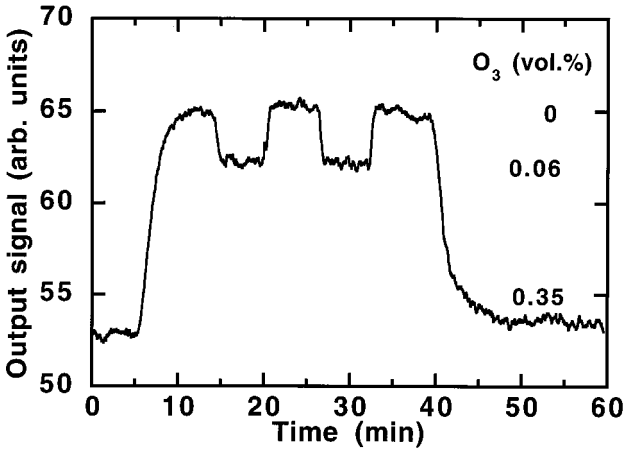

Figure 6. Dynamic response of the exposed-cladding ozone sensor.

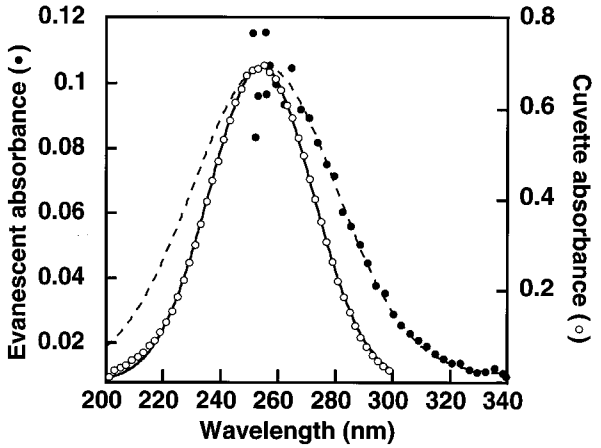

Figure 7. Comparison of absorption spectra of 0.35 vol % ozone obtained in the transmission (○) and evanescent-wave (●) modes. Gaussian fits according to eq 3: transmission spectrum fit (solid line) and evanescent-wave spectrum fit (dashed line).

tion range, a linear calibration was observed with a slope of $2.8 \times 10^{-1} \pm 2 \times 10^{-2}$ and intercept $-1 \times 10^{-3} \pm 2 \times 10^{-3}$ (mean ± SD, $n = 5$). The lowest concentration of ozone used in these experiments (0.06 vol %) yielded $S/N = 9.7$, where S is the analytical signal in the presence of ozone and N is the root-mean-square noise for the sensor in oxygen. The detection limit at $S/N = 3$ is therefore 0.02 vol %. The relative standard deviation (RSD) over the range of determined ozone concentrations (0.06−0.35 vol %) was 4−15%. The detection limit and RSD could both be improved by performing double-beam measurements to compensate for the drift in the optoelectronic components and by using mass-flow controllers to improve the stability of ozone generation. The sensor exhibited no noticeable change in response over two months of experiments.

The response of the sensor is completely reversible, as is illustrated in Figure 6. The sensor response times when exposed to 0.35 vol % ozone and pure oxygen were 10 and 8 min, respectively. The response time of the sensor in this experiment was limited by the rate at which the gas could be changed in the sample chamber. In this study, a gas flow of 0.1 L/min was employed to generate the requisite ozone concentration and was responsible for flushing the ozone generator, gas lines, and the sample chamber. At the smallest examined ozone concentration (0.06 vol %), 0.9 L/min gas flow was used, and the sensor response was 4−5 times shorter due to the accelerated gas mixture replacement. Although further studies of the sensor dynamic response were not performed because of the slow purge rate of the sample chamber, the sensor response time appears to be about 1 min, controlled by the diffusion kinetics of ozone.

An attempt was made to collect an evanescent-wave absorption spectrum of ozone with the exposed-cladding sensor. However, the low transmission of the optical fiber below 250 nm resulted in the determination of only the red-side wing of the Hartley absorption band. Figure 7 compares the absorption spectra of 0.35 vol % ozone collected with the evanescent-wave sensor and with the absorption cuvette. These spectral profiles were fitted to a Gaussian line shape for comparison of their peak positions and bandwidths:

$$A = A_{max} \exp[-\ln 2\ (\lambda - \lambda_{max})^2/(\Delta\lambda)^2] \qquad (3)$$

where A_{max} is the absorbance at the peak of the absorption band, λ_{max} is the wavelength at the absorption peak, and $\Delta\lambda$ is the absorption band half width at half-maximum (hwhm).

Table 1. Parameters of the Gaussian Fit (Eq 3) of the Hartley Absorption Band of Ozone

absorption spectrum	peak position, λ_{max} (nm)	band hwhm for red-side wing of absorptn profile, $\Delta\lambda$ (nm)	corr coeff, R
cuvette absorbance	254.0[a]	21.2	0.997
	253.9[b]	20.2	0.999
	254.2[c]	20.6	0.999
evanescent absorbance	255.2[a]	29.4	0.994

[a] Calculated from Figure 7. [b] Calculated from Figure VI-12(b) of ref 16. [c] Calculated from Figure 2. Measurements performed using a 3-m-long PCS optical fiber as an optical-fiber link.

Parameters of the Hartley band (λ_{max}, $\Delta\lambda$) collected with the evanescent-wave sensor and with the absorption cuvette are compared in Table 1. The data indicate that the shift in the peak position of the evanescent-wave absorption spectrum is within the range predicted by theory.[38] However, the red-side wing of the evanescent-wave spectrum appeared to be broader than predicted.[38] This 50% band broadening might be caused by the interaction of chemisorbed ozone with the fiber core.

Anomalous dispersion does not contribute to the observed sensor signal. Even at the maximum ozone concentration used in this study (0.35 vol %), the imaginary part n_2* of the complex refractive index[1] is at most 1×10^{-6} at the 254-nm peak of the Hartley band[39] (absorption coefficient 134 atm^{-1} cm^{-1}). According to the Kramers−Kronig relation between the real and imaginary parts of the complex refractive index in the vicinity of a Gaussian absorption peak,[38] the change Δn_{2max} in the real part of the complex refractive index is a function of the imaginary part n_2*; the ratio $\Delta n_{2max}/n_2* = 0.6$ holds for a wide range of n_2*.[38] For an absorption band as strong as $n_2* = 1 \times 10^{-6}$, the maximum change in the real part of the complex refractive index Δn_{2max} is only 6×10^{-7} refractive index unit (RIU). This variation in refractive index

(38) Potyrailo, R. A.; Ruddy, V. P.; Hieftje, G. M. *Appl. Opt.* **1996**, *35*, 4102−4111.
(39) Griggs, M. *J. Chem. Phys.* **1968**, *49*, 857−859.

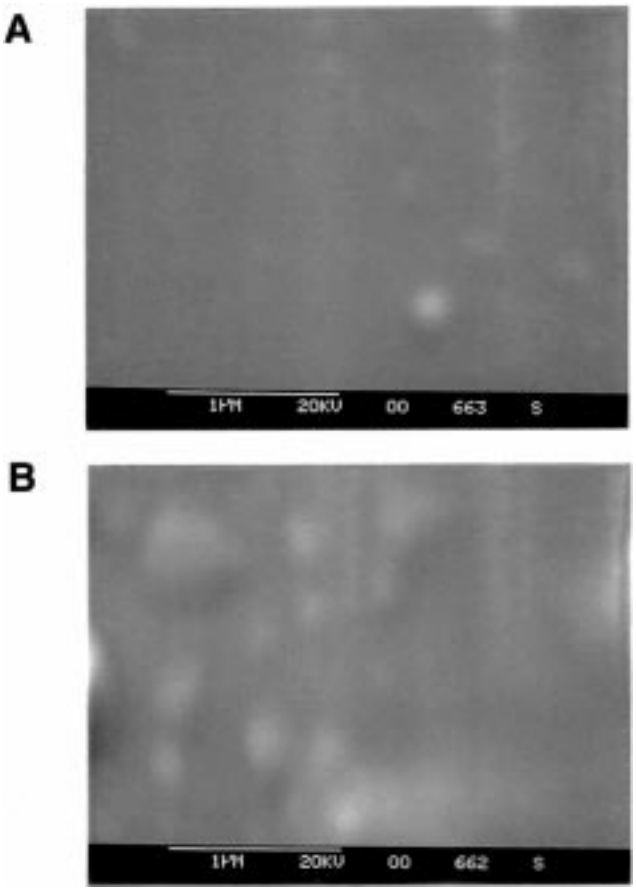

Figure 8. Scanning electron microscope images of a bare silica fiber core: (A) before and (B) after exposure to ozone for 200 h. The bar at the bottom of each picture is 1 μm.

is more than 1 order of magnitude less than the typical resolution ($\sim 10^{-5}$ RIU) of an evanescent-wave optical waveguide refractometric sensor.[40,41]

Bare-Silica Core Sensor. The bare-silica core sensor exhibited a response similar to that of the exposed-cladding sensor. However, concerns arose early about its long-term stability. A gradual drop in sensor response occurred after several tens of hours of exposure to ozone. Examination of the surface of the fiber core performed by scanning electron microscopy revealed the formation of bumps with typical dimensions of 100−300 nm (cf. Figure 8). The size of these features (which are most likely adsorbed dust nanoparticles) was comparable to the penetration depth of the probe near-UV evanescent wave. Thus, these bumps can effectively scatter the near-UV light and attenuate the amplitude of the evanescent wave. In addition to the rapid surface contamination, aging of the silica surface exposed to moisture in the ambient air and to ozone could also lead to signal loss. It is known that nucleophilic attack by water causes disruption of Si−O−Si linkages on the silica-fiber surface, leading to formation of microcracks, which may result in premature fracture.[42] Furthermore, the activation energy of the reaction of water with silica is a function of the stress applied to the fiber,[43] which is, or course, raised when the fiber is coiled.

CONCLUSIONS

Multimode low-cost PCS optical fibers have been used for the first time as ATR elements for the detection of species absorbing in the near-UV.[15] The feasibility of this approach was demonstrated by the construction of ozone sensors for industrial applications.

Application of unclad silica-core optical fibers for near-UV evanescent-wave analysis can be complicated by problems associated with rapid contamination and aging of the bare fiber surface. As a result of surface contamination, the amplitude of the evanescent field fades, causing a loss in analytical signal of a near-UV sensor more rapidly than it does in a sensor operating at longer wavelengths. Also, the combined effect of moisture, adsorbed species, and mechanical stress induced in the coiled fiber can cause rapid aging of the bare sensing surface.

An attractive solution for both of these problems is to protect the sensing surface with an analyte-permeable membrane that has a low optical attenuation in the near-UV. Fortunately, PCS fibers can be employed directly for this purpose. The analyte permeability properties of silicone are much better than those of most other fiber-cladding materials such as poly(methyl methacrylate) or fluorinated polymers,[44] thereby ensuring fast sensor response. Thus, a gas-permeable hydrophobic silicone cladding not only protects the silica fiber core from degradation but also provides a reliable and robust medium for the evanescent field of the near-UV radiation propagating in the fiber core. Importantly for the present application, silicone proved to be a stable material upon exposure to high concentrations of ozone.[22] It was successfully used previously as a material for ozone-permeable membranes to protect silica gel surfaces from the desensitizing effect of moisture.[28]

Evanescent-wave UV detection of ozone offers important advantages over the conventional UV transmission technique. First, detection of ozone in water with a PCS fiber-based sensor can eliminate signal drift caused by turbidity and water coloration from ionic species, because the silicone fiber cladding protects the sensing interface and serves as an ion-impermeable membrane. Second, evanescent-wave measurements of high ozone concentrations in water and air[23] are preferable to conventional UV transmission determinations since the latter would require submillimeter cells. The use of such short-path length cells leads to problems of rapid clogging and a variable optical path length in aggressive environments.[45,46]

For practical applications, the sensor could be simplified and miniaturized by using compact components such as a miniature deuterium lamp, a miniaturized battery-powered PMT in a TO-5 transistor can, and an interference filter. In such practical situations, the matter of interferences must also be considered. For example, in an environment that contains interfering UV-

(40) Cole, C. F.; Hill, G. M.; Adams, A. J. *J. Am. Oil Chem. Soc.* **1994**, *71*, 1339−1342.
(41) Johnstone, W.; Fawcett, G.; Yim, L. W. K. *IEE Proc.: Optoelectron.* **1994**, *141*, 299−302.
(42) Blyler, L. L., Jr.; Eichenbaum, B. R.; Schonhorn, H. In *Optical Fiber Telecommunications*; Miller, S. E., Chynoweth, A. G., Eds.; Academic Press: New York, 1979, 299−341.
(43) Kao, C. K. *Optical Fiber Systems: Technology, Design, and Applications*; McGraw-Hill Book Co.: New York, 1982.
(44) Brandrup, J., Immergut, E. H. Eds. *Polymer Handbook*, 3rd ed.; Wiley-Interscience: New York, 1989.
(45) Peramunage, D.; Forouzan, F.; Licht, S. *Anal. Chem.* **1994**, *66*, 378−383.
(46) Giggenbach, W. *Inorg. Chem.* **1971**, *10*, 1333−1338.

absorbing species, it would be possible to use a PC card-type UV−visible CCD spectrometer and a multiwavelength calibration routine. An interference might also arise from the adsorption of foreign species onto the surface of the fiber, an occurrence that would alter the refractive index of the surrounding medium. However, this adsorption would cause only a baseline shift, which could readily be differentiated from the absorption peak of the analyte.[9] Moreover, the thickness of such an adsorbed layer would be negligible compared with the penetration depth of the evanescent field, which is of the order of the wavelength of the probe light. As a result, the adsorbed layer would attenuate the evanescent wave to only a very small degree.

Other types of UV transparent optical fibers could potentially be employed for near-UV evanescent-wave sensing. For example, ozone detection with sapphire fibers might offer greater initial stability of the sensor response, since sapphire is less reactive with ozone. The tradeoffs, however, are in the lack of commercially available plastic-clad sapphire optical fibers and the high cost of bare-core sapphire fibers.

Of course, the use of near-UV evanescent-wave sensing with multimode PCS optical fibers can be easily extended to the detection of other, less reactive, UV-absorbing compounds. For example, the UV detection of neutral species in aqueous solution is currently under study; results will be reported in a forthcoming publication.

ACKNOWLEDGMENT

This work was supported in part by the National Institutes of Health through Grant GM 53560. R.A.P. gratefully acknowledges the support from Boehringer Mannheim Corporation for a Summer Research Fellowship.

Received for review August 26, 1997. Accepted February 13, 1998.

AC970942V